

Angular dependent magnetoresistance with twofold and fourfold symmetries in A-type antiferromagnetic $\text{Nd}_{0.45}\text{Sr}_{0.55}\text{MnO}_3$ thin film

Y. Q. Zhang,^{a)} H. Meng, X. W. Wang, X. Wang, H. H. Guo, Y. L. Zhu, T. Yang, and Z. D. Zhang

Shenyang National Laboratory for Materials Science, Institute of Metal Research and International Centre for Materials Physics, Chinese Academy of Sciences, 72 Wenhua Road, Shenyang 110016, People's Republic of China

(Received 3 August 2010; accepted 5 October 2010; published online 28 October 2010)

The angular dependent magnetoresistance (AMR) of $\text{Nd}_{0.45}\text{Sr}_{0.55}\text{MnO}_3$ thin film epitaxially grown on SrTiO_3 (001) is examined at different temperatures and magnetic fields. Twofold and fourfold symmetric AMR and a transition between them are observed under two different measurement modes and are found to be dependent on temperature and/or strength of a magnetic field. In comparison with AMR occurring in other systems, we believe that the twofold/fourfold symmetric AMR observed here corresponds to different spin-canted states induced by the magnetic field at certain temperatures below the Néel temperature. © 2010 American Institute of Physics.

[doi:10.1063/1.3507262]

Anisotropic magnetoresistance or so-called angular dependent magnetoresistance (AMR) phenomenon has been attracting much attention due to its potential applications in the magnetic recording industry. Recently, anomalous behavior in AMR was reported for ferromagnetic (FM) manganites, such as $\text{La}_{0.65}\text{Ca}_{0.35}\text{MnO}_3$ and $\text{La}_{0.75}\text{Ca}_{0.25}\text{MnO}_3$.^{1,2} In conventional FM alloys, AMR is positive and decreases with decreasing magnetization or increasing temperature; but AMR in manganites is negative with a nonmonotonic temperature dependence showing a peak close to its Curie temperature (T_C). When a film becomes thinner, lattice mismatch-induced strain modifies the magnitude of AMR dramatically. AMR in some systems exceeds 100% and can even change sign.³ In the charge-orbital-ordered $\text{Sm}_{0.5}\text{Ca}_{0.5}\text{MnO}_3$ films,⁴ AMR was found below the charge order temperature under a magnetic field larger than 6 T. When a magnetic-field induced insulator-metal transition occurs, the magnitude of AMR decreases dramatically and the sign further changes from $\cos^2 \theta$ -to $\sin^2 \theta$ -dependence. In a word, the AMR reported previously in manganites is related to strong couplings between spin, charge, orbital and lattice degrees of freedom, which are all tuned by strain. However, current theories of AMR in FM materials cannot explain the origin of AMR in manganites.

In this paper, AMR at different temperatures and magnetic fields in epitaxial $\text{Nd}_{0.45}\text{Sr}_{0.55}\text{MnO}_3$ (NSMO) film grown on SrTiO_3 (STO)(001) is investigated with modes A and B. Remarkably different from AMR reported previously,¹⁻⁴ both twofold and fourfold symmetric AMR are observed in our films at certain temperatures below its Néel temperature of 282 K, depending on the strength of the magnetic field. The amplitude of AMR peak in mode A is larger than that in mode B.

Bulk NSMO is a $d_{x^2-y^2}$ orbital order, metallic, A-type antiferromagnetic (AFM) oxide in which FM layers stack with AFM couplings.⁵ A paramagnetic (PM)-AFM transition occurs in bulk NSMO at its Néel temperature ($T_N=225$ K), and it becomes metallic below T_N until 80 K, then an insu-

lator again. Below T_N , the $d_{x^2-y^2}$ orbital order favors double exchange interaction in the a-b plane FM layers while it weakens superexchange interaction between FM layers along the c axis leading to highly anisotropic transport properties. Namely, there is two-dimensional metallic behavior along the a-b plane FM layer (although it becomes an insulator again below 80 K), and insulator behavior occurs along AFM couple direction (c axis).

6 nm NSMO films were grown on STO (100) by pulsed laser deposition. The coherent epitaxial growth, crystal structure and lattice parameters of the film were confirmed by a high-resolution transmission electron microscope (HRTEM) and x-ray diffraction (XRD). The AMR measurements on the as-grown films were performed using a physical property measurement system (PPMS) equipped with two different sample rotators providing two measurement modes [as illustrated in Figs. 3(a) and 4(a)]. In mode A, the current (I) is along the rotation axis of the film plane, the magnetic field (B) is always perpendicular to the current and θ (in degrees) is the angle between the magnetic field and the film plane with 0° defined as follows: $B \perp$ film plane. In mode B, both the magnetic field and current are in the a-b plane direction, θ is the angle between the magnetic field and current with 0° defined as follows: $B \perp I$. In both modes the film was rotated from 0° to 360° while the resulting AMR was being recorded.

Figure 1 shows the cross-sectional HRTEM image of the

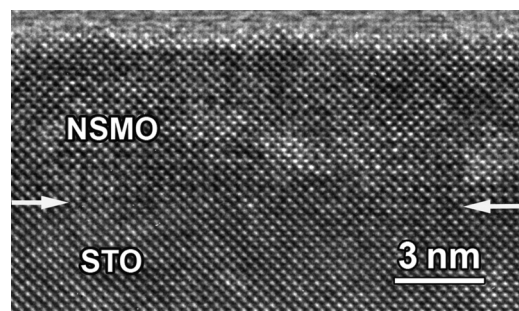


FIG. 1. Cross-sectional HRTEM image of 6 nm NSMO film grown on STO.

^{a)}Electronic mail: yqzhang@imr.ac.cn.

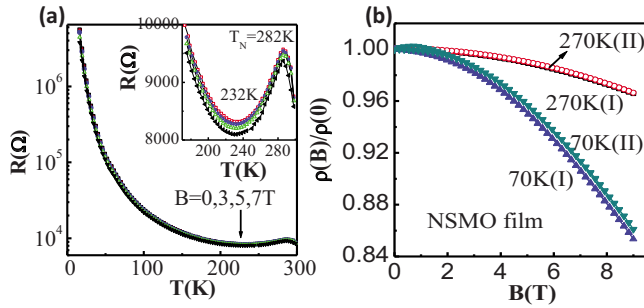


FIG. 2. (Color online) (a) Temperature dependence of the in-plane resistance of 6 nm NSMO film at different magnetic fields. (b) Magnetic field dependence of $\rho(B)/\rho(0)$ at 270 and 70 K: (I) mode B ($\theta=90^\circ$); (II) mode A ($\theta=0^\circ$).

6 nm NSMO film grown on STO. It can be seen that the NSMO film grows coherently with the substrate without misfit dislocations along the interface. XRD data shows that, compared with bulk, the in-plane lattice parameter of NSMO is increased while the out-of-plane lattice parameter is decreased, leading to a tetragonal lattice distortion with $c/a=0.9656$. Such a tetragonal distortion favors A-type AFM ordering⁶ where spins are aligned ferromagnetically within the planes and coupled antiferromagnetically between neighboring planes.

Figure 2(a) shows the temperature dependence of the resistance in the a-b plane of the as-grown film under different magnetic fields. It is clearly seen from the inset that when the temperature decreases, the resistance first increases, reaching a maximum at a temperature corresponding to its Néel temperature ($T_N=282$ K), then decreases until 232 K, and finally increases again. This indicates that metallic behavior appears below T_N ($=282$ K) until 232 K, and then it becomes an insulator again. We define the insulator-metal transition temperature as T_N in our film since PM-AFM transition is accompanied by an insulator-metal transition in the a-b plane direction. This is quite similar to the bulk material,⁵ except for a higher T_N than the bulk value (225 K). This is also in agreement with the tetragonal lattice distortion mentioned above. Under the application of magnetic fields of 3, 5, and 7 T, the resistance is almost unchanged, compared to that at zero field. It implies that the $d_{x^2-y^2}$ orbital order AFM state is very stable in this film.

Below its Néel temperature T_N ($=282$ K), no obvious AMR is observed in the films with a magnetic field smaller than 5 T in both measurement modes. Figures 3(a) and 3(b) show the angular dependence of the observed AMR at 270 K, 240 K, 150 K, and 70 K at a magnetic field of 5 T and 9 T, respectively, in measurement mode A.

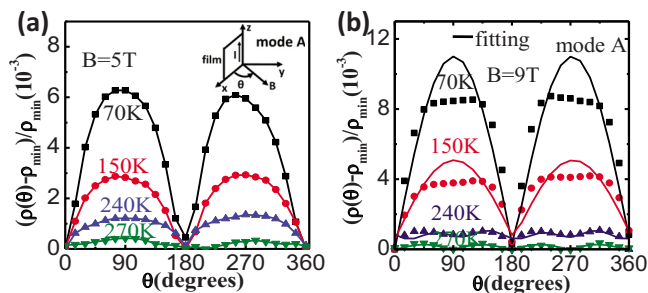


FIG. 3. (Color online) [(a) and (b)] Angular dependence of the observed AMR at 270 K, 240 K, 150 K, and 70 K under magnetic fields of 5 T and 9 T, respectively, in measurement mode A.

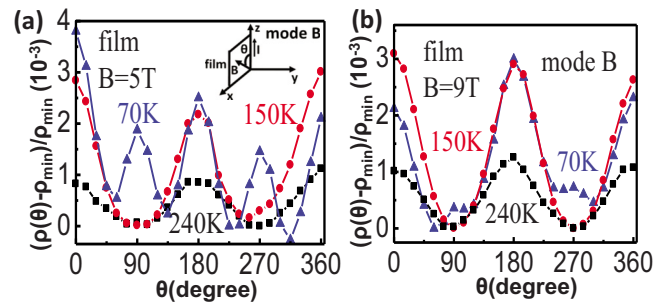


FIG. 4. (Color online) [(a) and (b)] Angular dependence of the observed AMR at 240 K, 150 K, and 70 K under magnetic fields of 5 T and 9 T, respectively, in measurement mode B.

9 T, respectively, in mode A. Here, $AMR(\theta)=[\rho(\theta)-\rho(\min)]/\rho(\min)$, where $\rho(\min)$ is the minimum among the angular dependent resistivities. Below T_N , $AMR(\theta)$ shows twofold symmetry ($\sin^2 \theta$ dependence) with peaks at 90° and 270° , and valleys at 0° and 180° at 5 T. When the applied magnetic field is larger than 5 T, at 270 K, a deviation from the twofold symmetry starts to appear with a broadening of the peaks near 90° and 270° and the appearance of an additional set of peaks, finally showing fourfold symmetry at 9 T. With decreasing temperature, at a constant field of 9 T, the fourfold symmetry weakens and becomes a mixture of fourfold and twofold symmetries at 240 K. And it eventually changes into twofold symmetry at 150 and 70 K. An interesting thing is that the fittings of the curves (solid line) at 150 and 70 K actually are a $\sin^2(\theta)$ dependence form with a lack of peak sharpness, and indicates that the spin canted states have already become saturated when the magnetic field reaches a 45° angle and remain unaffected (resistivity remains constant) by the continued movement of the films a-b plane into the magnetic field until 135° where it begins to decrease again.

The angular dependence of AMR at 240 K, 150 K, and 70 K at magnetic fields of 5 T and 9 T in the mode B is shown in Figs. 4(a) and 4(b), respectively. In contrast to mode A, no AMR is observed at 270 K even at 9 T and $AMR(\theta)$ shows a $\cos^2 \theta$ dependence (although still with twofold symmetry) with peaks at 0° and 180° , and valleys at 90° and 270° at 240 and 150 K at both 5 and 9 T. While decreasing the temperature from 150 K, at 5 T, a deviation from the twofold symmetry starts with a broadening of the peaks near 0° and 180° and an additional set of peaks appears, thus showing fourfold symmetry at 70 K. Moreover, at a constant temperature (e.g., 70 K), the fourfold symmetry becomes weaker with a further increase in the magnetic field and changes into twofold symmetry at 9 T.

AMR phenomenon in our film is very different from the previous reports where no fourfold symmetric AMR was observed in FM and charge-ordered manganite films. We note that our AMR measurement method in mode B is the same as that used by Chen *et al.*⁴ in CE type (the FM ordering along the zigzag chain and AFM ordering along the direction perpendicular to the chain) charge ordered $Sm_{0.5}Ca_{0.5}MnO_3$ films where, when a metal-insulator transition in R-T curve is induced by a magnetic field of 13 T, AMR decreases dramatically at 80 K (metal) as compared to that at 150 K (insulator). In our case (in the a-b plane direction), although the magnitude of AMR in the insulator state (150 and 70 K) is also larger than that in the metallic state (240 and 270 K)

under 5 T and 9 T, respectively, it is field independent [seen clearly from Figs. 4(a) and 4(b)]. The reason is that, as introduced above, the NSMO film is A-type $d_{x^2-y^2}$ orbital ordered metallic antiferromagnet where no charge order has ever been reported and so-called metallic behavior only appears in the a-b plane due to $d_{x^2-y^2}$ orbital order. In addition, when an applied magnetic field is larger than the critical field at a fixed temperature below T_N , A-type $d_{x^2-y^2}$ orbital ordered AFM material can be changed into an orbital disordered FM metal. However, in our film with a thickness of 6 nm, the maximum applied field of 9 T is not enough to cause such a transition to occur below T_N . This can be seen from the $\rho(B)/\rho(0)$ -B curve at 270 and 70 K in mode B ($\theta=90^\circ$) and mode A ($\theta=0^\circ$) in Fig. 2(b) I and II, respectively. Here, the resistivity at 270 and 70 K decreases monotonically with an increasing magnetic field and no sudden drop can be found. This differs with what happens as the AFM-FM transition occurs under a critical magnetic field in bulk. But, no field less than 3 T may induce an orientation of spins leading to a spin-canting state accompanied by a negative magnetoresistance [as seen from Fig. 2(a)]. In bulk NSMO,⁵ a large negative magnetoresistance is observed over a wide temperature region below T_N . Especially, along the AFM coupling direction (c axis), the magnetic field forcedly aligns opposite spins in the adjacent a-b plane to its direction, resulting in the spin canting. It is understood that the two-and/or fourfold symmetric AMR observed at 5 and 9 T in our film results from different spin canting states induced by the magnetic field. This is similar in nature to AFM $\text{Nd}_{2-x}\text{Ce}_x\text{CuO}_4$,⁷ where fourfold symmetric AMR occurred in different AFM structures because the magnetic field is able to rotate the direction of spins relative to the crystallographic axis. Moreover, it was reported in Ref. 8 that a variation in AMR symmetry with temperature arises from the subtle changes of the spin structure at a fixed magnetic field, namely, AMR shows a twofold symmetry at high temperature but a sixfold symmetry below a certain temperature corresponding to a different spin structure.⁸ Therefore, we believe that our observed twofold/fourfold symmetric AMR and transition between them, correspond to different spin-canted structures.

We find that the amplitudes in the AMR peaks in measurement modes A and B show dramatic differences at low temperatures (e.g., 150 and 70 K). The amplitude in the AMR peak is equal to the value of $[\rho(\text{max})-\rho(\text{min})]$ in Figs. 3 and 4. This is related with the $d_{x^2-y^2}$ orbital order in our film. As introduced above, $d_{x^2-y^2}$ orbital order favors metallic transport, although it is an insulator at low temperature in the a-b plane and there is an insulator transport property along the c axis. That is to say, $d_{x^2-y^2}$ orbital order confines elec-

trical charge transport to the a-b plane. This is also confirmed by Fig. 2(b) where it is seen that at 270 or 70 K, the resistivity is smaller in mode B ($\theta=90^\circ$) (I) than in mode A ($\theta=0^\circ$) (II). It is evident that, in our measurement mode B, no larger in-plane resistivity anisotropy [i.e., no larger difference between $\rho(\text{max})$ and $\rho(\text{min})$] at 5 or 9 T is expected due to electrical charge being confined in the a-b plane. However, in mode A, larger resistivity anisotropy is expected due to the change of angle between the a-b plane and magnetic field. So, the amplitude of AMR peak in mode A is found to be larger than that in mode B. In mode B, especially at 70 K, it is observed that the amplitudes of the 0° , 180° , and 360° peaks are not only larger than those at 90° and 270° but are different from one another as seen in Fig. 4(b). Lorentz force effects alter the path of the charge carriers and should lower the conductivity and increase the AMR. For our case, the Lorentz force effects can be excluded, as are significant for $\omega_c\tau > 0.1$ where ω_c is the cyclotron frequency and τ is the scattering time, and for manganites $\omega_c\tau$ is small.⁴ The noted amplitude difference may be due to inhomogeneous field-induced domain wall effects.

In summary, the AMR with twofold and fourfold symmetries, dependent on temperature and magnetic field strength, is observed in A-type AFM NSMO thin film. The AMR possibly originates from magnetic-field induced spin-canting states at certain temperatures below its Néel temperature.

This work has been supported by the National Natural Science Foundation under Grant Nos. 50802098 and 11004201, the National Basic Research Program Grant No. 2010CB934603, and the Ministry of Science and Technology of China.

¹M. Bibes, V. Laukhin, S. Valencia, B. Martinez, J. Fontcuberta, O. Yu Gorbenco, A. R. Kaul, and J. L. Martinez, *J. Phys.: Condens. Matter* **17**, 2733 (2005).

²J. D. Fuhr, M. Granada, L. B. Steren, and B. Alascio, *J. Phys.: Condens. Matter* **22**, 146001 (2010).

³M. Egilmez, M. M. Saber, A. I. Mansour, R. C. Ma, K. H. Chow, and J. Jung, *Appl. Phys. Lett.* **93**, 182505 (2008).

⁴Y. Z. Chen, J. R. Sun, T. Y. Zhao, J. Wang, Z. H. Wang, B. G. Shen, and N. Pryds, *Appl. Phys. Lett.* **95**, 132506 (2009).

⁵H. Kuwahara, T. Okuda, Y. Tomioka, A. Asamitsu, and Y. Tokura, *Phys. Rev. Lett.* **82**, 4316 (1999).

⁶R. Maezono, S. Ishihara, and N. Nagaosa, *Phys. Rev. B* **57**, R13993 (1998).

⁷X. H. Chen, C. H. Wang, G. Y. Wang, X. G. Luo, J. L. Luo, G. T. Liu, and N. L. Wang, *Phys. Rev. B* **72**, 064517 (2005).

⁸C. H. Wang, X. H. Chen, G. Wu, T. Wu, H. T. Zhang, J. L. Luo, G. T. Liu, and N. L. Wang, *Phys. Rev. B* **74**, 172507 (2006).